IEEE Access
Multidisciplinary | Rapid Review | Open Access Journal

Received March 9, 2019, accepted March 24, 2019, date of publication April 1, 2019, date of current version April 18, 2019.

Digital Object Identifier 10.1109/ACCESS.2019.2908388

Sequential and Iterative Distributed Model Predictive Control of Multi-Motor Driving Cutterhead System for TBM

XIAOFENG YANG[1], LANGWEN ZHANG[1], (Member, IEEE), WEI XIE[1], AND JUNFENG ZHANG[2,3]

[1]College of Automation Science and Technology, South China University of Technology, Guangzhou 510641, China
[2]School of Automation, Hangzhou Dianzi University, Hangzhou 310018, China
[3]Key Laboratory of System Control and Information Processing, Ministry of Education of China, Shanghai 200240, China

Corresponding author: Langwen Zhang (aulwzhang@scut.edu.cn)

This work was supported in part by the National Natural Science Foundation of China under Grant 61803161 and Grant 61873314, in part by the Key Laboratory of Advanced Process Control for Light Industry Ministry of Education under Grant APCLI1801, in part by the Yangfan Innovative & Entepreneurial Research Team Project of Guangdong Province under Grant 2016YT03G125, in part by the Innovative Research Team Project of Jiangmen under Grant 2017TD03, in part by the Science and Technology Planning Project of Guangdong Province under Grant 2018B010108001, Grant 2017B090914001, Grant 2017A040405023, Grant 2017A040403064, Grant 2017B090901040, and Grant 2017B030306017, in part by the Science and Technology Program of Guangzhou under Grant 201707010152, in part by the Natural Science Foundation of Guangdong Province under Grant 2017A030313385 and Grant 2018A030310371, and in part by the Fundamental Research Funds for the Central Universities under Grant 2018A030310371.

ABSTRACT In this paper, we investigate the robust control of multi-motor driving cutterhead system for tunnel boring machines (TBMs) with distributed model predictive control (MPC). By analyzing the working procedures of the induction motor, coupling, reduction gear box, and spur gear, a dynamical model of cutterhead system is established. The model is then represented into a state-space model with additional loads. A sequential and iterative distributed MPC algorithm is established for optimizing the input torques for the driving motors. To design the distributed MPC, the whole system is decomposed into several subsystems according to the distribution of input torques. The future system outputs are predicted by using the system model and the distributed MPC optimizes the input sequence at each time instant in a recursive fashion. The model errors are corrected by comparing the actual outputs and predicted outputs. A sequential and iterative algorithm is proposed to coordinate the distributed MPC controllers. Finally, simulations are carried out to validate the distributed MPC algorithm on torque optimization of cutterhead system in TBMs.

INDEX TERMS Tunnel boring machine, cutterhead system, distributed MPC, iterative.

I. INTRODUCTION

TBM is a large-scale underground equipment which is used to excavate tunnels to provide a capacity for water transfer, railway tunnels and mine boring. TBM excavation method is high safety, rapid excavation and low manual labor [1] and can reduce the cost of the project [2]. TBM has become one of the most common tools for tunneling [3]. As shown in Fig. 1, the main components of a typical TBM are the cutterhead driving system, support and thrust system, auxiliary system. Among them, the cutterhead system undertakes the task of excavating rocks and soil [4], which plays an important role in TBM.

The cutterhead driving system is generally driven by three-phase AC asynchronous induction motor [5]. Motor drive system is effective in mechanical design, installation and maintenance. If one of the motor angular velocity is lower or higher than the other motor angular velocity for a long time, the motor will be overheating and probably get damaged [6]. To achieve stability of cutterhead driving, angular velocity control is of crucial importance [7]. Induction motors are difficult to control and not suitable for high dynamic performance applications because of their complex nonlinear dynamics [8]. Vector control provides decoupled control of the flux magnitude and the torque producing current, which is commonly used in asynchronous motor [9]. The local control of induction motor is guaranteed by the high efficient vector control. However, for the cutterhead driving

The associate editor coordinating the review of this manuscript and approving it for publication was Liang Hu.

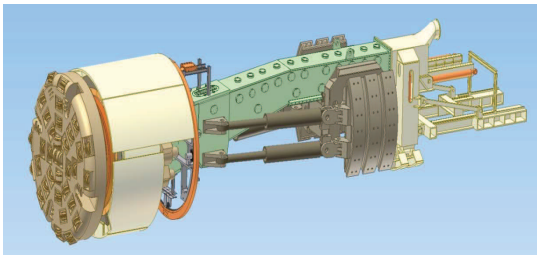

FIGURE 1. Structure diagram of the TBM.

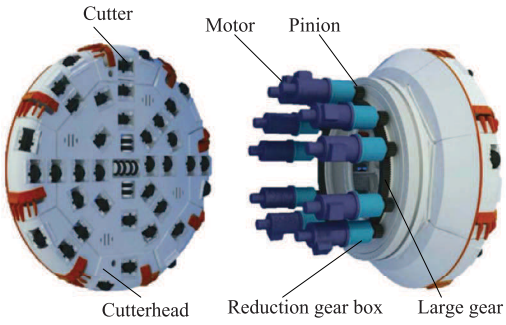

FIGURE 2. The structure of cutterhead driving system.

system, due to the varying working environments (such as disturbance, weakness zones or hard/soft rock), inevitable uncertainties and loads change often emerge and has great effects on the performance. It is difficult to decide the torque settings for the vector control under the complex working environments, which is critical for improving the tunneling efficiency of TBM. To the best of our knowledge, the control of TBM cutterhead driving system has not yet attracted wide attentions.

For a cutterhead driving system, model uncertainties and disturbances are inevitable due to the complex tunneling environment, which can severely affect the control performance. MPC is an effective control scheme in practice since it is being able to handle multi-variable, uncertain and constrained systems [10]. The applications of MPC include the chemical processes, power systems, urban traffic systems and irrigation canals [11]. In mechanical design area, MPC also has attracted wide attentions [12]–[14]. However, the applications are limited to simple systems, for example, an effective MPC algorithm was designed for robot manipulators with integral sliding modes generation in [15]. Generally, the diameter of the cutterhead is more than five meters and more than thirty motors are used to drive the cutterhead. The control of these motor-driving cutterhead systems could be very complex. For the large-scale systems, the computation time could be a challenge since the MPC controller is solved online for each sampling time [16]. To address this problem, different kinds of high effective MPC methods have been proposed, i.e., the explicit MPC [17], the decentralized MPC [18] and the distributed MPC [19].

Decentralized MPC is one of the approaches to reduce the computational complexity, in which subsystem design local controller independently of each other [20]–[22]. Information exchange is not allowed during the controller design process. Nevertheless, it is known that such a completely decentralized MPC may result in unacceptable control performance, especially when the couplings between subsystems are strong [23]. The centralized and the decentralized MPC are the two design extremes for the control of large-scale systems [24]. The centralized MPC structure takes into account all possible interactions and the decentralized MPC ignores them partially or completely. Additionally, both the decentralized and the centralized MPC structures allow no information communication between subsystems [25].

An alternative control method for the large-scale systems is distributed MPC structure [26]–[29]. The distributed MPC can preserve the topology of centralized MPC and flexibility of decentralized MPC and at the same time may offer a nominal closed-loop stability guarantee [30]. The distributed MPC techniques require decomposing the entire plants into subsystems and solving each subsystem with coordination to reach a global control performance. The performance of the cooperative distributed MPC algorithm is better than fully decentralized MPC when the interactions among the subsystems are strong [18], [31], [32]. With the ability to deal with system constraints, model uncertainties and disturbance, it can be expected that distributed MPC can be used to control the cutterhead system of TBM effectively. In general, there are two different approaches to handle the distributed MPC problems. The first one is based on tube based control [33]. This approach attempts to reach the centralized MPC performance via communicating with other subsystems [34]. The second approach is known as parallel distributed MPC, in which each subsystem cooperates to obtain a consensus [35]. For example, an effective distributed MPC algorithm was presented for nonlinear systems with asynchronous and delayed measurements in [36]; A distributed MPC was investigated for local and global constrained systems in [37]; For the communication for the distributed MPC, the tolerant to communication loss was discussed in [38] and [39].

In this paper, a distributed control structure is presented for multi-motor driving cutterhead system of TBM, which integrates sequential and iterative distributed MPC strategy with torque allocation technique. The paper presents a detailed and complete dynamic modeling process, and a state-space linear model form is further derived. To design the distributed MPC, the future system outputs are predicted by using the system model; Based on the predicted outputs, the MPC controller optimizes the input sequence at each time instant in a recursive fashion; The model errors are corrected by comparing the actual outputs and predicted outputs. Finally, a distributed MPC structure is proposed for optimizing the motor torques to address synchronous control scheme.

The remainder of this paper is organized as follows: in Section 2, modeling procedures of TBM cutterhead system are presented; The sequential and iterative distributed

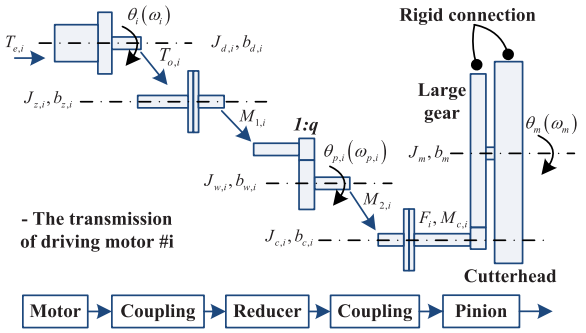

FIGURE 3. Transmission of driving motor $i(i = 1, \cdots, n)$.

MPC structure is proposed in Section 3. The simulation results are given in Section 4 and Section 5 concludes this paper.

II. MODELING OF TBM CUTTERHEAD SYSTEM

In this section, a linear dynamic model of TBM cutterhead driving system is built by analyzing the procedures of induction motor, coupling, reduction gear box and spur gear. The model description follows from [5] and forms the background of the control problem. The cutterhead geometry for driving motor i is given in Fig. 3.

The multiple active pinions mesh the center passive large gear, which is multi-gear transmission structure. Each active pinion is driven by an induction motor. The electrical magnetic torque of the induction motors is synthesized via multi-gear transmission structure. The large gear and cutterhead have the same rotary angular speed since the large gear and the cutterhead are rigidly connected. The induction motor's speed is reduced by the reducer to amplify the output torque.

For driving motor $i(i = 1, \cdots, n)$, the electrical magnetic torque balance equations can be established as:

$$T_{e,i} = J_{d,i}\ddot{\theta}_i + b_{d,i}\dot{\theta}_i + T_{o,i} \tag{1}$$

$$T_{o,i} = J_{z,i}\ddot{\theta}_i + b_{z,i}\dot{\theta}_i + M_{1,i} \tag{2}$$

where $T_{e,i}$ is the induction motor electrical magnetic torque of motor i; $T_{o,i}$ is the output torque of motor i; $M_{1,i}$ is the input torque of reducer i; θ_i denotes the angular displacement of ith motor; $J_{d,i}$ denotes the induction motor rotor inertia; $b_{d,i}$ denotes the induction motor rotor viscous damping; $J_{z,i}$, $b_{z,i}$ denote the inertia and viscous damping between ith motor and ith coupling respectively.

Substituting (2) into (1), we have:

$$T_{e,i} = J_{d,z,i}\ddot{\theta}_i + b_{d,z,i}\dot{\theta}_i + M_{1,i} \tag{3}$$

where $J_{d,z,i} = J_{d,i} + J_{z,i}$, $b_{d,z,i} = b_{d,i} + b_{z,i}$.

The input-output relationships of the ith reducer can be described as follows:

$$\theta_i = q\theta_{p,i} \tag{4}$$

$$M_{2,i} = qM_{1,i} \tag{5}$$

where q is the transmission ratio of reducer i; $\theta_{p,i}$ denotes the angular displacement of ith after the reducer i.

The torque balance equation of the ith pinion is given as:

$$M_{2,i} = J_{c,i}\ddot{\theta}_{p,i} + b_{c,i}\dot{\theta}_{p,i} + M_{c,i} \tag{6}$$

where $J_{c,i} = J_{p,i} + J_{w,i}$, $b_{c,i} = b_{p,i} + b_{w,i}$; $J_{p,i}$ denotes the ith active pinion inertia; $b_{p,i}$ denotes the ith active pinion viscous damped; $J_{w,i}$ denotes the inertia of ith coupling between ith reducer and ith pinion; $b_{w,i}$ denotes the ith active pinion viscous dampe; $M_{c,i}$ denotes the elastic mesh torque.

The elastic mesh torque between pinion i and large gear is:

$$M_{c,i} = k_{t,i}\varphi_i\left(\theta_{p,i} - \theta_m i_{m,i} + \beta_i\right) + c_{t,i}\varphi_i\left(\dot{\theta}_{p,i} - \dot{\theta}_m i_{m,i} - r_i^{-1}\dot{e}_i(t)\right) \tag{7}$$

where $k_{t,i}$, $c_{t,i}$ respectively denote the mesh torque coefficients of ith pinion and gear; θ_m denotes the angular displacement of large gear; $i_{m,i}$ is the gear transmission ratio; $k_{t,i}$, $c_{t,i}$ and $e_i(t)$ are period time-varying parameters that can be expressed as the Fourier series [5]

$$\begin{cases} k_{t,i} &= k_0 + \sum_{i=1}^{\infty} k_i \cos(2\pi i f_z t + \phi_i^k) \\ c_{t,i} &= c_0 + \sum_{i=1}^{\infty} c_i \cos(2\pi i f_z t + \phi_i^c) \\ e_i(t) &= e_0 + \sum_{i=1}^{\infty} e_i \cos(2\pi i f_z + \phi_i^e) \end{cases} \tag{8}$$

where k_0, c_0 and e_0 are average mesh stiffness, mesh damping ratio and transmission error respectively; f_z is the meshing frequency; ϕ_i^k, ϕ_i^c, ϕ_i^e represent the phase angles of mesh stiffness, mesh damping ratio and transmission error; and [5]

$$\varphi_i = \begin{cases} 1, & \left|\theta_{p,i} - i_{m,i}\theta_m - \frac{e_i(t)}{r_i}\right| \geq \Delta_i \\ 0, & \left|\theta_{p,i} - i_{m,i}\theta_m - \frac{e_i(t)}{r_i}\right| < \Delta_i \end{cases} \tag{9}$$

$$\beta_i = \begin{cases} -\frac{e_i(t)}{r_i} - \Delta_i, \theta_{p,i} - i_{m,i}\theta_m - \frac{e_i(t)}{r_i} \geq \Delta_i, \\ 0, -\Delta_i < \theta_{p,i} - i_{m,i}\theta_m - \frac{e_i(t)}{r_i} < \Delta_i \\ -\frac{e_i(t)}{r_i} + \Delta_i, \theta_{p,i} - i_{m,i}\theta_m - \frac{e_i(t)}{r_i} \leq -\Delta_i \end{cases} \tag{10}$$

where $\Delta_i = \frac{\Delta_b^i}{r_i}$ represents the relative backlash; Δ_b^i is the backlash of the ith gear pair.

The torque balance equations of large gear are obtained as:

$$M_m = J_m\ddot{\theta}_m + b_m\dot{\theta}_m + T_L \tag{11}$$

$$M_m = i_{m,i}\left(M_{c,1} + M_{c,2} + \cdots + M_{c,n}\right) \tag{12}$$

where T_L is total load torque.

The load torque has great influence on the cutterhead driving system. During the operation, if the load torque is larger than the maximum designed driving torque of the cutterhead, the cutterhead components could be damaged.

From (1)-(12), we have:

$$\begin{aligned} qT_{e,i} = &\left(q^2 J_{d,z,i} + J_{c,i}\right)\ddot{\theta}_{p,i} + \left(q^2 b_{d,z,i} + b_{c,i}\right)\dot{\theta}_{p,i} \\ &+k_{t,i}\varphi_i\left(\theta_{p,i} - \theta_m i_{m,i} + \beta_i\right) \\ &+c_{t,i}\varphi_i\left(\dot{\theta}_{p,i} - \dot{\theta}_m i_{m,i} - r_i^{-1}\dot{e}_i(t)\right) \end{aligned} \tag{13}$$

where $i = 1, 2, \cdots, n$ and

$$J_m\ddot{\theta}_m + b_m\dot{\theta}_m + T_L = \sum_{i=1}^{n} i_{m,i}\Big\{k_{t,i}\varphi_i\left(\theta_{p,i} - \theta_m i_{m,i} + \beta_i\right) + c_{t,i}\varphi_i\Big(\dot{\theta}_{p,i} - \dot{\theta}_m i_{m,i} - r_i^{-1}\dot{e}_i(t)\Big)\Big\} \tag{14}$$

Due to the period time-varying parameters $k_{t,i}$, $c_{t,i}$, $e_i(t)$ and the multi-sector nonlinear factors φ_i, β_i, the nonlinear models (13)-(14) are not directly suitable for a model based controller design, as e.g., MPC. To reduce the model complexity, the following assumptions are considered [5], [40]:

(i) The backlash is generally very small and has litter effect on the motor output. When the backlash of the ith gear pair $\Delta_b^i = 0$, we have $\varphi_i = 1$ and $\beta_i = -\frac{e_i(t)}{r_i}$;

(ii) The period time-varying parameters $k_{t,i}$, $c_{t,i}$ and e_i are simplified with the average values, that are $k_{t,i} = k_0$, $c_{t,i} = c_0$, $e_i(t) = e_0$ and $\dot{e}(t) = 0$.

It has been shown in [41] that the variation range of backlash parameter is only between $[-0.2\ 0.2]\mu m$, compared with the diameter of the driving motor (generally 30 centimeters), these nonlinearities are neglectable if we design robust controller for the cutterhead system.

Let us denote the variables $u = \left[T_{e,1} \cdots T_{e,n}\ T_L\right]^T$, $x = \left[\theta_{p,1} \cdots \theta_{p,n}\ \theta_m\ w_{p,1} \cdots w_{p,n}\ w_m\right]^T$, $y = \left[w_{p,1} \cdots w_{p,n} w_m\right]^T$, the state space form of cutterhead system model is obtained as follows:

$$\begin{aligned}\dot{x} &= \begin{bmatrix}A_{11} & A_{12}\\ A_{21} & A_{22}\end{bmatrix}x + \begin{bmatrix}B_{11}\\ B_{21}\end{bmatrix}u\\ y &= \begin{bmatrix}C_{11} & C_{12}\end{bmatrix}x\end{aligned} \tag{15}$$

where $A_{11} = B_{11} = C_{11} = 0_{(n+1)\times(n+1)}$ and

$$A_{12} = C_{12} = I_{(n+1)\times(n+1)},$$

$$A_{21} = \begin{bmatrix}\frac{-k_{t,1}\varphi_1}{J_1} & \cdots & 0 & \frac{k_{t,1}\varphi_1 i_{m,1}}{J_1}\\ \vdots & \ddots & \vdots & \vdots\\ 0 & \cdots & \frac{-k_{t,n}\varphi_n}{J_n} & \frac{k_{t,n}\varphi_n i_{m,n}}{J_n}\\ \frac{i_{m,1}k_{t,1}\varphi_1}{J_m} & \cdots & \frac{i_{m,n}k_{t,n}\varphi_n}{J_m} & \frac{-\sum_{b=1}^{n} i_{m,b}^2 k_{t,b}\varphi_b}{J_m}\end{bmatrix},$$

$$A_{22} = \begin{bmatrix}\frac{\alpha_1}{J_1} & \cdots & 0 & \frac{\beta_1}{J_1}\\ \vdots & \ddots & \vdots & \vdots\\ 0 & \cdots & \frac{\alpha_n}{J_n} & \frac{\beta_n}{J_n}\\ \frac{\beta_1}{J_m} & \cdots & \frac{\beta_n}{J_m} & \frac{-\left(\sum_{b=1}^{n} i_{m,b}^2 c_{t,b}\varphi_b + b_m\right)}{J_m}\end{bmatrix},$$

$$\alpha_i = -b_i - c_{t,i}\varphi_i,\ \beta_i = c_{t,i}\varphi_i i_{m,i},$$

TABLE 1. Parameter values of cutterhead system.

Parameter	Value
q	165.3
$b_{d,i}$	$0.225kg \cdot m^2/rad/s$
r_m	$1.0m$
$J_{c,i}$	$0.1767kg \cdot m^2$
J_m	$56.93\ kg \cdot m^2$
$k_{t,i}$	$10^5 N \cdot m/rad$
b_m	$0.921kg \cdot m^2/rad/s$
$c_{t,i}$	$10^2 N \cdot m/rads^{-1}$
r_i	0.2 m
$b_{c,i}$	$0.105kg \cdot m^2/rad/s$
$J_{d,i}$	$2.1\ kg \cdot m^2$

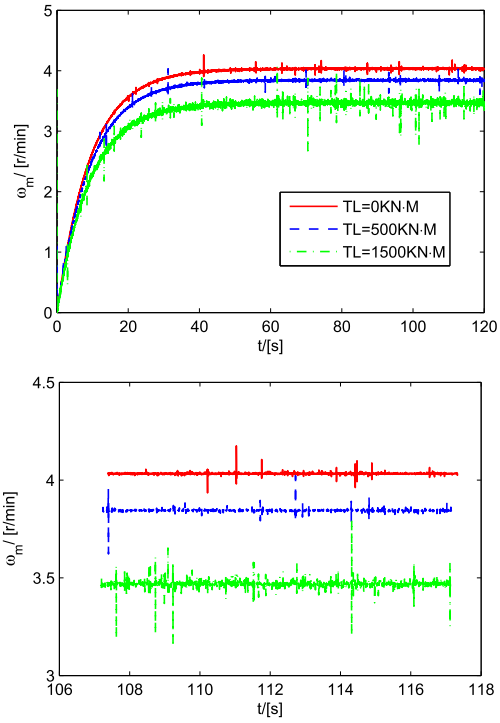

FIGURE 4. Dynamic responses of ω_m under different loads $T_L = 0\ kN \cdot m$, $500\ kN \cdot m$ and $1500\ kN \cdot m$.

$$J_i = J_{d,i}q^2 + J_{c,i}, b_i = b_{d,i}q^2 + b_{c,i}, i = 1, \cdots, n,$$

$$B_{21} = \begin{bmatrix}\frac{q}{J_1} & \cdots & 0 & 0\\ \vdots & \ddots & \vdots & \vdots\\ 0 & \cdots & \frac{q}{J_n} & 0\\ 0 & \cdots & 0 & \frac{1}{J_m}\end{bmatrix}.$$

Then, the generalized linear dynamic model of the cutterhead system is established.

To test the established system model, testing simulations are given. Since the load torque has great influence on the cutterhead driving system, different loads $T_L = 0$ kN·m, $T_L = 500$ kN·m, $T_L = 1500$ kN·m are considered respectively. The torques are set as constant $T_{e,i} = 900$ N·m and $n = 4$. The parameters are selected from [5] and shown in Table 1. The output seed of motors and cutterhead are shown in Figs. 4 and 5. The open-loop responses show that

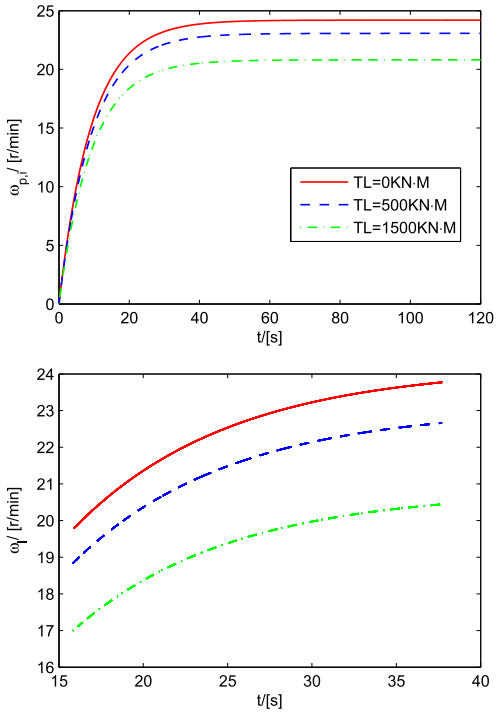

FIGURE 5. Dynamic responses of $\omega_{p,i}$ under different loads $T_L = 0\ kN \cdot m$, $500\ kN \cdot m$ and $1500\ kN \cdot m$.

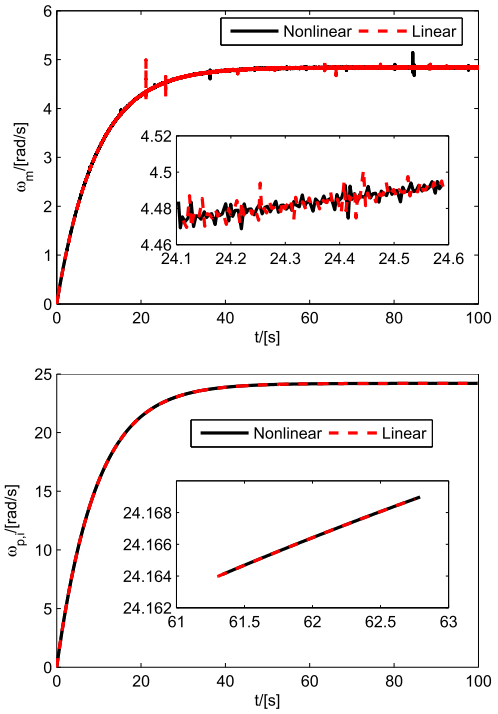

FIGURE 6. Comparisons for nonlinear and linear models of cutterhead system in TBM.

the different loads will results in different steady output speeds. The outputs of the nonlinear system and linear model are compared under $T_L = 100$ kN·m. The result is tested in Fig. 6, demonstrating that the responses of the two models are very similar, which means that the model (15) can be used for optimizing the torques if we design a robust controller.

Remark 1: It is noted that the torques of the induction motors $T_{e,i}, i = 1, \cdots, n$ should be strictly limited to ensure the safety of the boring processes. The system will be shut down immediately when the torque exceeds 80% of the nominal torque $T^N_{e,i}$ for more than five seconds or exceeds $T^N_{e,i}$. Thus, the constraints are mainly on the inputs $T_{e,i}$. That is $0 \leq T_{e,i} \leq 0.8 * T^N_{e,i}$ with $i = 1, \cdots, n$.

Remark 2: The control problem of the cutterhead system becomes: how to decide the electrical magnetic torques of the induction motors $T^*_{e,i}, i = 1, \cdots, n$, so that the cutterhead system can successfully track the expected w^*_m subject to the load disturbances and system constraints.

Remark 3: Due to the uncertain excavation environment underground, the loads acting the cutterhead change frequently. The random load disturbances are described as $T_L = 90 * [1 + 0.25 * (2 * rand - 1)]$ kN· m, which means that the load changes around 90 kN· m with ±25% fluctuant of load disturbances. The load disturbances make the speed tracking control critical difficult. A robust control method is necessary for the TBM cutterhead system to handle the robustness issue under complex excavating environment.

Remark 4: The dimensions of the cutterhead system model will increase with increasing number of the driving motors. The control of the motor-driving cutterhead system could be very complex. The computation time could be a challenge if we directly apply the MPC method. Thus, we consider the tracking problem of cutterhead system with distributed MPC. The advantages are: (1) The computational burden will be reduced by designing distributed MPC controllers compared with the centralized MPC; (2) The flexibility and robustness of the control system will be improved.

Remark 5: A multi-layer control structure is considered with distributed MPC tracking layer and PID control layer: (1) the expected output speed w^*_m of the cutterhead system is given by the Real Time Optimization (RTO) layer; (2) the electrical magnetic torques of the induction motors $T^*_{e,i}, i = 1, \cdots, n$ are optimized by distributed MPC in the supervisory control layer and given as the setpoints of the regulatory control layer; (3) the regulatory control layer (local PID control) of induction motors is designed for tracking the setpoints received from distributed MPC.

III. CONTROL STRAGEGY

The TBM cutterhead system control problem can be reduced to control of discrete-time, linear system:

$$\begin{cases} x_{k+1} = (A + \Delta A)x_k + Bu_k + GT_L + d(k) \\ y_k = Cx_k \end{cases} \tag{16}$$

where $x = \left[\theta_{p,1} \cdots \theta_{p,n}\ \theta_m\ \ w_{p,1} \cdots w_{p,n}\ w_m\right]^T$ denotes the angles and the speeds of the cutterhead and cutterhead; $u = \left[T_{e,1} \cdots T_{e,n}\right]^T$ denotes the toques of the driving motors; ΔA is the model uncertainty and $d(k)$ represents the

unmeasured disturbances as defined in Remark 3; $C = [C_{11}\ C_{12}]$; $A = \begin{bmatrix} A_{11} & A_{12} \\ A_{21} & A_{22} \end{bmatrix}$, and

$$B = \begin{bmatrix} 0 & \cdots & 0 \\ \vdots & \ddots & \vdots \\ 0 & \cdots & 0 \\ \frac{q}{J_1} & \cdots & 0 \\ \vdots & \ddots & \vdots \\ 0 & \cdots & \frac{q}{J_n} \\ 0 & \cdots & 0 \end{bmatrix}, G_L = \begin{bmatrix} 0 \\ \vdots \\ 0 \\ 0 \\ \vdots \\ 0 \\ \frac{1}{J_m} \end{bmatrix}.$$

The nominal system model is written as

$$\begin{cases} \tilde{x}_{k+1} = A\tilde{x}_k + B\tilde{u}_k + GT_L \\ \tilde{y}_k = C\tilde{x}_k \end{cases} \tag{17}$$

The nominal system model is used to predict the future dynamics of the system. Taking the model uncertainties and disturbances into account, a robust feedback control law $u_k = F_k x_k$ should be given. At each time instant, all the control inputs are computed simultaneously. The conventional MPC algorithm requires on-line optimization, in which computational complexity can become a challenge when applying MPC to the cutterhead systems with fast response times. Motivated by the deficiency of the centralized MPC algorithm, we propose a distributed MPC scheme for the cutterhead system in TBMs.

A. DISTRIBUTED MPC STRATEGY

In distributed MPC scheme, model (16) is represented as:

$$x_{i,k+1} = Ax_{i,k} + B_i u_{i,k} + \sum_{j=1(j\neq i)}^{M} B_j u_{j,k} + GT_L + L_{i,c}\left(y_{i,k} - y_{i,k|k-1}\right) \tag{18}$$

where B_i is decided by $B_i = \left[B_{i,(i-1)m_i+1}\ \cdots\ B_{i,im_i}\right]$. In (18), $B_{i,(i-1)m_i+1}$ represents the $[(i-1)m_i+1]$th column of B. $u_{i,k} \in R^{m_i}$ represents the ith input. $u_{j,k} \in R^{m_j}$ denotes the neighbour jth inputs. For system (18), the following performance index is considered:

$$J_{i,k} = \sum_{l=0}^{N-1}\left(\left\|x_{i,k+l|k}\right\|_Q^2 + \left\|u_{i,k+l|k}\right\|_{R_i}^2\right) + \sum_{l=0}^{N-1}\sum_{j=1(j\neq i)}^{M}\left\|u_{j,k+l}\right\|_{R_j}^2 + P_{i,f}\left(x_{i,k+N|k}\right) \tag{19}$$

where $Q \in R^n$, $R_i \in R^{m_i}$ and $R_j \in R^{m_j}$ respectively denote the weighting matrices of states, ith inputs, and jth inputs. The term $P_{i,f}\left(x_{i,k+N|k}\right) = x_{i,k+N|k}^T P_{i,k} x_{i,k+N|k}$ with $P_{i,k} = P_{i,k}^T > 0$ is a suitably chosen terminal cost coefficient to ensure the closed-loop stability [42].

Minimizing $J_{i,k}$ without imposing other restrictions is not attractive, since it requires an infinite number of degrees of $u_{i,k+l|k}$, $\forall l \geq 0$. To avoid this problem, the parameterization of the input is switched to a state feedback law beyond the control horizon N:

$$u_{i,k+l|k} = K_i x_{i,k+l|k}, \forall l \geq N \tag{20}$$

The input constraints as described in Remark 1 can be described as follows:

$$u_{i,k+l|k} \in \mathbb{U}_i, i \in [1, M], l \in [0, N-1] \tag{21}$$

where $\mathbb{U}_i$ is equal to polyhedral set

$$W_i u_{i,k+l|k} \leq h_i, i \in [1, M], l \in [0, N-1] \tag{22}$$

where $W_i = \begin{bmatrix} I \\ I \end{bmatrix}$, $e = \begin{bmatrix} 0.8 * T_{e,i}^N \\ 0 \end{bmatrix}$. Then, N step forward predictions of states are obtained as follows:

$$X_{i,k|k} = \Psi_i x_{i,k|k} + \Gamma_i U_{i,k|k} + \sum_{j=1(j\neq i)}^{M} \Gamma_j U_{j,k}^{\star} + \Gamma_G T_{k|k} + L_{i,c}\left(y_{i,k} - y_{i,k|k-1}\right) \tag{23}$$

where $L_{i,c} = \left[I_{ny_i}, \cdots, I_{ny_i}\right]_{n_{y_i}\times N}^T$; $U_{j,k}^{\star}$ refer to the control action received from the neighbor subsystem and

$$X_{i,k|k} = \begin{bmatrix} x_{i,k+1|k} \\ \vdots \\ x_{i,k+N|k} \end{bmatrix}, \quad U_{i,k|k} = \begin{bmatrix} u_{i,k|k} \\ \vdots \\ u_{i,k+N-1|k} \end{bmatrix},$$

$$U_{j,k|k}^{\star} = \begin{bmatrix} u_{j,k|k} \\ \vdots \\ u_{j,k+N\text{-}1\ |k} \end{bmatrix}, \Psi_i = \begin{bmatrix} A \\ A^2 \\ \vdots \\ A^{H_P} \end{bmatrix},$$

$$\Gamma_i = \begin{bmatrix} B_i & 0 & \cdots & 0 \\ AB_i & B_i & \cdots & 0 \\ \vdots & \vdots & \vdots & \vdots \\ A^{N\text{-}1}B_i & A^{N\text{-}2}B_i & \cdots & B_i \end{bmatrix},$$

$$\Gamma_j = \begin{bmatrix} B_j & 0 & \cdots & 0 \\ AB_j & B_j & \cdots & 0 \\ \vdots & \vdots & \ddots & \vdots \\ A^{N\text{-}1}B_j & A^{N\text{-}2}B_j & \cdots & B_j \end{bmatrix},$$

$$\Gamma_G = \begin{bmatrix} G & 0 & \cdots & 0 \\ AG & G & \cdots & 0 \\ \vdots & \vdots & \ddots & \vdots \\ A^{N\text{-}1}G & A^{N\text{-}2}G & \cdots & G \end{bmatrix}.$$

At time interval k, obtain the ith subsystem's input by solving the following optimization problem:

$$\min_{U_{i,k}} J_{i,k|k} = \left\|X_{i,k|k}\right\|_{\hat{Q}}^2 + \left\|U_{i,k|k}\right\|_{\hat{R}_i}^2 + \sum_{j=1(j\neq i)}^{M}\left\|U_{j,k}^{\star}\right\|_{R_j}^2 + x_{i,k|k}^T Q x_{i,k|k}$$

$$s.t.\ X_{i,k|k} = \Psi_i x_{i,k|k} + \Gamma_i U_{i,k|k} + \sum_{j=1(j\neq i)}^{M} \Gamma_j U_{j,k}^{\star}$$

$$
\begin{aligned}
&+\Gamma_G T_{k|k}+L_{i,c}\left(y_{i,k}-y_{i,k|k-1}\right)\\
&u_{i,k+l|k}\in\mathbb{U}_i,\ l\in[0,N-1]\\
&x_{i,k+N|k}\in\mathbb{Z},\ \mathbb{Z}\subset\mathbb{X}
\end{aligned}
\tag{24}
$$

where $\hat{Q}=diag(\underbrace{Q,\cdots,Q}_{N},P_{i,k})$, $\hat{R}_i=diag(\underbrace{R_i,\cdots,R_i}_{N})$.

Lemma 1: By solving the following quadratic programming optimization (QP) problem, the distributed MPC controller can be obtained:

$$
\begin{aligned}
&\min_{U_{i,k|k}}\frac{1}{2}U_{i,k|k}^T H_i U_{i,k|k}+f_i U_{i,k|k}\\
&s.t.\ W_i u_{i,k+l|k}\le h_i,\ l\in[0,N-1]
\end{aligned}
\tag{25}
$$

where the positive define matrix H_i has the following form

$$
H_i=\Gamma_i^T\hat{Q}\Gamma_i+\hat{R}_i \tag{26}
$$

and matrix f_i has the following form

$$
\begin{aligned}
f_i=\Gamma_i^T\hat{Q}\big[&\Psi_i x_{i,k|k}+\sum_{j=1(j\neq i)}^{M}\Gamma_j U_{j,k}^{\star}\\
&+\Gamma_G T_{k|k}+L_{i,c}\left(y_{i,k}-y_{i,k|k-1}\right)\big]
\end{aligned}
\tag{27}
$$

For the system without constraints, an analytical solution can be obtained as follows:

$$
U_{i,k|k}^{*}=\left(\Gamma_i^T\hat{Q}\Gamma_i+\hat{R}_i\right)^{-1}\Gamma_i^T\hat{Q}\Pi_{i,j,k} \tag{28}
$$

The first input in $U_{i,k|k}^{*}$ can be represented as $u_{i,k|k}^{*}=L_i U_{i,k|k}^{*}$, where $L_i=[I_{m_i}\underbrace{0\cdots0}_{N-1}]$.

Proof: Substituting (23) into $J_{i,k|k}$, we have:

$$
\begin{aligned}
J_{i,k}=&\left(\Pi_{i,j,k}+\Gamma_i U_{i,k|k}\right)^T\hat{Q}\left(\Pi_{i,j,k}+\Gamma_i U_{i,k|k}\right)\\
&+U_{i,k|k}^T\hat{R}_i U_{i,k|k}+\sum\nolimits_{j=1(j\neq i)}^{M}U_{j,k}^{\star\,T}\hat{R}_j U_{j,k}^{\star}\\
=&\,\Pi_{i,j,k}^T\hat{Q}\Gamma_i U_{i,k|k}+U_{i,k|k}^T\Gamma_i^T\hat{Q}\Pi_{i,j,k}\\
&+U_{i,k|k}^T\Gamma_i^T\hat{Q}\Gamma_i U_{i,k|k}+U_{i,k|k}^T\hat{R}_i U_{i,k|k}+x_{k|k}^T Q x_{k|k}\\
&+\Pi_{i,j,k}^T\hat{Q}\Pi_{i,j,k}+\sum\nolimits_{j=1(j\neq i)}^{M}U_{j,k}^{\star\,T}\hat{R}_j U_{j,k}^{\star}
\end{aligned}
\tag{29}
$$

Then, the optimization problem (24) is represented as a standard quadratic programming optimization problem (25). This completes the proof. ■

Generally, we consider the tracking control of cutterhead system, the control objective is to steer the output speed of cutterhead to the time-varying expected speed ω_m^r under different excavating conditions. Then, the optimization problem (25) is generally transformed into the tracking MPC with the tracking performance index

$$
\begin{aligned}
\tilde{J}_{i,k}=&\sum_{l=1}^{H_P}\left\|\left(y_{k+l|k}-y_{k+l|k}^r\right)\right\|_{Q_y}^2+\sum_{l=0}^{N-1}\left\|\Delta u_{i,k+l|k}\right\|_{R_{i,y}}^2\\
&+\sum_{l=0}^{N-1}\sum_{j=1,j\neq i}^{M}\left\|\Delta u_{j,k+l|k}\right\|_{R_{j,y}}^2
\end{aligned}
\tag{30}
$$

where $Q_y\in R^{n_y}$, $R_{i,y}\in R^{m_i}$, $R_{j,y}\in R^{m_j}$ denote the weighting matrices of states and inputs, respectively; $y_{k+l|k}^r$ represents the set-points of the cutterhead system, generally $y_{k+l|k}^r=\omega_{k+l|k}^r$. The prediction horizon H_P is typically chosen in a way that the main dynamic behavior of the system can be covered. H_P step forward predictions of states can be represented as follows:

$$
\begin{aligned}
Y(i,k|k)=&\,\Psi_y x_{i,k|k}+\Gamma_{i,y}u_i(k-1)+\Theta_{i,y}\Delta U(i,k\,|k)\\
&+\sum_{j=1,j\neq i}^{M}\left[\Gamma_{j,y}u_j(k-1)+\Theta_{j,y}\Delta U(j,k|k)\right]\\
&+\Gamma_G^y T_{k|k}+L_y\left(y_k-y_{k|k-1}\right)
\end{aligned}
\tag{31}
$$

where $L_y\left(y_k-y_{k|k-1}\right)$ accounts for unmeasured disturbance and the difference between the nominal model (17) and the real model (16); $L_y=\left[I_{n_y},\cdots,I_{n_y}\right]_{n_y\times H_P}^T$ and

$$
Y(i,k|k)=\begin{bmatrix}y_{i,k+1|k}\\ \vdots\\ y_{i,k+H_P|k}\end{bmatrix},
$$

$$
\Delta U(i,k|k)=\begin{bmatrix}\Delta u_{i,k|k}\\ \vdots\\ \Delta u_{i,k+N-1|k}\end{bmatrix},
$$

$$
\Psi_y=\begin{bmatrix}CA\\ CA^2\\ \vdots\\ CA^{H_P}\end{bmatrix},
$$

$$
\Gamma_{i,y}=\begin{bmatrix}CB_i\\ C(AB_i+B_i)\\ \vdots\\ \sum_{l=1}^{H_P-1}CA^lB_i\end{bmatrix},
$$

$$
\Theta_{i,y}=\begin{bmatrix}CB_i & \cdots & 0\\ C(AB_i+B_i) & \cdots & 0\\ \vdots & \vdots & \vdots\\ \sum_{l=1}^{H_P-1}CA^lB_i & \cdots & \sum_{l=1}^{H_P-N}CA^lB_i\end{bmatrix},
$$

$$
\Gamma_G^y=\begin{bmatrix}CG & 0 & \cdots & 0\\ CAG & CG & \cdots & 0\\ \vdots & \vdots & \ddots & \vdots\\ CA^{H_P-1}G & CA^{H_P-N-2}G & \cdots & CG\end{bmatrix},
$$

and $\Delta U_{j,k|k}$, $\Gamma_{j,y}$, $\Theta_{j,y}$ can be obtained by replacing i with j in $\Delta U_{i,k|k}$, $\Gamma_{i,y}$, $\Theta_{i,y}$, respectively.

At time interval k, the control inputs can be obtained by solving the following optimization problem

$$
\min_{\Delta U_i(k|k)}\bar{J}_i,\ s.t.\ (31)\text{ and }(22) \tag{32}
$$

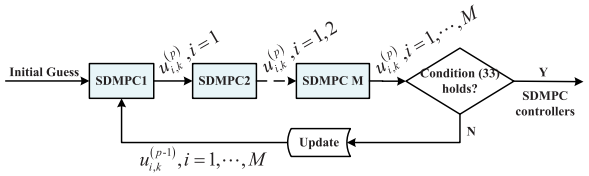

FIGURE 7. Sequential and iterative distributed MPC.

where $\bar{J}_i = \|Y(i,k|k) - Y_r(k|k)\|^2_{Q_y} + \|\Delta U_i(k|k)\|^2_{\hat{R}_{i,y}} + \sum_{j=1,j\neq i}^{M} \|\Delta U_j(k|k)\|^2_{\hat{R}_{j,y}}$ and

$$\hat{Q}_y = \begin{bmatrix} Q_y & \cdots & 0 \\ \vdots & \ddots & \vdots \\ 0 & \cdots & Q_y \end{bmatrix}, \hat{R}_{i,y} = \begin{bmatrix} R_{i,y} & \cdots & 0 \\ \vdots & \ddots & \vdots \\ 0 & \cdots & R_{i,y} \end{bmatrix},$$
$$Y_r(k|k) = \left[y_r^T(k+1|k) \cdots y_r^T(k+H_P)\right]^T.$$

B. SEQUENTIAL AND ITERATIVE ALGORITHM

Note that there are couplings in the (23) when solving the optimization problem (25). We introduce a sequential and iterative algorithm to coordinate the distributed MPC controllers. As shown in Fig. 7, Algorithm 1 is executed in sequential and iterative fashion for all subsystems. The upstream control input is $u_{i,k}^{up}$ is solved and transmitted to the downstream systems. For the downstream subsystems, the $u_{i,k}^{up}$ is treated as known input when solving the downstream control inputs $u_{i,k}^{down}$. The convergence of $u_{i,k}$ is checked with a pre-specified error tolerance $\epsilon_{i,k}$ when all the controllers are obtained. If the criteria are not satisfied, all the subsystems will update the new $u_{i,k}^{(p)}$ and repeat the above sequential procedure.

The computation time will increase with increasing iterations. Hence, there is a trade-off between computation time and the control performance. Compared with the parallel distributed MPC algorithms [28] and [35] in which all the feedback laws obtained at the same time, the proposed sequential and iterative method is more easy to achieve better control performance with less iterations. This is due to the fact that the controller $u_{i,k}^{down}$ of the downstream subsystems is solved not only based on the initial guesses, but also based on the real control input $u_{i,k}^{up}$ of upstream. However, the parallel distributed MPC are based on the initial guessed controllers of the neighbor subsystems.

Remark 6: The communications are required to transmit the control actions $U_{j,k|k}^{\star}$ of the neighbor subsystems at each time interval. Based on the neighbor $U_{j,k|k}^{\star}$, the agent is able to solve the local controllers. A key component of the distributed MPC is the exchange of controller information at each time interval. The exchange is required for one or several times at every time interval.

C. FEASIBILITY AND STABILITY

Next, the feasibility and the stability are discussed.

Algorithm 1 (Distributed MPC Algorithm)

Offline. At initial time, given an initial feasible $U_{i,k|k}^{\star}$ with $i \in [1, M]$ by optimizing a centralized MPC algorithm; given the state weighting matrices Q, input weighting matrices $R_1, \cdots, R_M$ and the maximum iteration $p_{m,k}$. Let iteration $p = 1$ and repeat the following procedure for each subsystem i at each time interval.

Online.

1: All subsystems: share the measured $x_{ii,k}$ of subsystem i;
2: Each subsystem solve (24) or (32) in sequential to obtain $U_{i,k|k}$ or $\Delta U_{i,k|k}$;
3: Let $u_{i,k}^{(p)} = u_{i,k}$ and check the convergence of $u_{i,k}$ with a pre-specified error tolerance $\epsilon_{i,k}$:

$$\left\| u_{i,k}^{(p)} - u_{i,k}^{(p-1)} \right\| \leq \epsilon_{i,k}, \ i = 1, 2, \cdots, M \tag{33}$$

If (33) or $p = p_{m,k}$ is satisfied, go to step 5; Otherwise, update the distributed controllers with $u_{i,k}^{*} = u_{i,k}^{(p)}$ and set $p = p + 1$, go to step 2;
4: The optimal control action $u_{1,k}, u_{2,k}, \cdots, u_{M,k}$ are applied to the plant.
5: Set $k = k + 1$ and go to step 1.

Theorem 1: The distributed MPC controllers obtained by solving the Algorithm 1, can ensure the stability of the closed-loop system if $\{P_{i,f}(\cdot)\}$ satisfies

$$P_{i+1,f}([A + B_i K_i]\, x) - P_{i,f}(x) \leq -\|x\|^2_Q - \|K_i x\|^2_{R_i} \tag{34}$$

for $i = 1, \cdots, M$.

Proof: The feasibility is ensured if there exists a feasible solution at the initial time interval [43]. Let

$$u_{k+l|k}^{*} = \left[u_{1,k+l|k-1}^T \cdots u_{i,k+l|k}^{(*)T} \cdots u_{M,k+l|k-1}^T\right]^T \tag{35}$$

represents the optimal solution of (25), $x_{k+l|k}^{*}$ represents the corresponding state and $J_{i,k}^{*}$ denotes corresponding cost function at time k. A candidate input sequence at time interval $k+1$ is

$$\tilde{u}_{k+1|k} = \left[u_{1,k+1|k-1}^T \cdots u_{i,k+1|k}^{(*)T} \cdots u_{M,k+1|k-1}^T\right]^T$$

$\tilde{J}_{i+1,k+1}$ is used to denote the performance index at time interval $k+1$. Then, we get:

$$\begin{aligned} \tilde{J}_{i,k+1} - J_{i,k}^{*} = & \left\|K_i x_{x+N|k}\right\|^2_R \\ & + P_{i,f}\left((A + B_i K_i)\, x_{x+N|k}\right) - \left\|u_{i,k|k}^{*}\right\|^2_{R_i} \\ & - \sum_{j=1(j\neq i)}^{M} \left\|u_{j,k|k-1}\right\|^2_{R_j} \\ & - \left\|x_{k|k}^{*}\right\|^2_Q - P_{i,f}\left(x_{x+N|k}\right) + \left\|x_{k+N|k}\right\|^2_Q \end{aligned} \tag{36}$$

Then, $\tilde{J}_{i,k+1} - J_{i,k}^{*} \leq 0$ if (34) holds. Optimization at the time interval $k+1$ will result in $J_{i,k+1}^{*} \leq \tilde{J}_{i,k+1}$. Thus, we have $J_{i,k+1}^{*} \leq J_{i,k}^{*}$. Since $J_{i,k}^{*} \geq 0$ for all k, we have

$J^*_{i,k+1} - J^*_{i,k} \to 0$ for $k \to \infty$. From (36) we can get $J^*_{i,k+1} - J^*_{i,k} \leq -\left\|u^*_{i,k|k}\right\|^2_{R_i} - \sum_{j=1(j\neq i)}^{M} \left\|u_{j,k|k-1}\right\|^2_{R_j} - \left\|x_{k|k}\right\|^2_{Q}$.

Thus, the controllers solved in Algorithm 1 can ensure the closed-loop stability if (34) holds. This ends the proof. ■

Condition (34) is a general condition to ensure the closed-loop stability of distributed MPC. We select

$$P_{i,f}\left(x_{i,k+N|k}\right) = x^T_{i,k+N|k} P_{i,k} x_{i,k+N|k} \tag{37}$$

where $P_{i,k} = P^T_{i,k} > 0$ is a suitably chosen terminal cost coefficient. If $P_{i,k}$ is the solution of the discrete-time periodic Riccati equation $P_{i,k} = A^T P_{i,k+1} A - A^T P_{i,k+1} B_{i,k} \nabla B^T_{i,k} P_{i,k+1} A + Q$, $\nabla = B^T_{i,k} P_{i,k+1} B_{i,k} + R_i$. Then, the condition (34) is automatically satisfied [42].

IV. SIMULATIONS

In this Section, we give simulations to test the effectiveness of the proposed distributed MPC with sequential and iterative coordination algorithm.

A. SIMULATION SETUP

It is assumed that there are four driving motors ($n = 4$). To derive the torque optimization for multi-motor driving cutterhead system of TBM using distributed MPC, model (16) is represented with system matrices: $A_{11} = B_{11} = C_{11} = 0_{5\times5}$, $A_{12} = C_{12} = I_{5\times5}$, $J_i = J_{d,i}q^2 + J_{c,i}$, $b_i = b_{d,i}q^2 + b_{c,i}$, $k_{t,i} = k_i r_i^2$, $c_{t,i} = c_i r_i^2$ and

$$A_{21} = \begin{bmatrix} \frac{-k_{t,1}}{J_1} & \cdots & 0 & \frac{i_{m,1}k_{t,1}}{J_1} \\ \vdots & \ddots & \vdots & \vdots \\ 0 & \cdots & \frac{-k_{t,4}}{J_4} & \frac{i_{m,4}k_{t,4}}{J_4} \\ \frac{i_{m,1}k_{t,1}}{J_m} & \cdots & \frac{i_{m,4}k_{t,4}}{J_m} & \frac{-\sum_{b=1}^{4} i^2_{m,b}k_{t,b}}{J_m} \end{bmatrix},$$

$$A_{22} = \begin{bmatrix} \frac{-(b_1+c_{t,1})}{J_1} & \cdots & 0 & \frac{c_{t,1}i_{m,1}}{J_1} \\ \vdots & \ddots & \vdots & \vdots \\ 0 & \cdots & \frac{-(b_n+c_{t,4})}{J_n} & \frac{c_{t,4}i_{m,4}}{J_4} \\ \frac{i_{m,1}c_{t,1}}{J_m} & \cdots & \frac{i_{m,4}c_{t,4}}{J_m} & \frac{-\left(\sum_{b=1}^{4} i^2_{m,b}c_{t,b}+b_m\right)}{J_m} \end{bmatrix},$$

$$B_{21} = \begin{bmatrix} \frac{q}{J_1} & \cdots & 0 & 0 \\ \vdots & \ddots & \vdots & \vdots \\ 0 & \cdots & \frac{q}{J_4} & 0 \\ 0 & \cdots & 0 & \frac{-1}{J_m} \end{bmatrix} \in R^{5\times5}$$

The driving system is decomposed into two subsystems based on the control inputs with subsystem 1: $\{T_{e,1}, T_{e,2}\}$ and subsystem 2: $\{T_{e,3}, T_{e,4}\}$. The corresponding input matrices

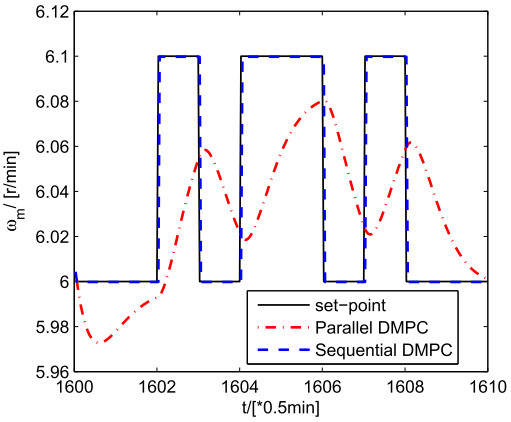

FIGURE 8. Output responses of driving motors under sequential distributed MPC and parallel distributed MPC.

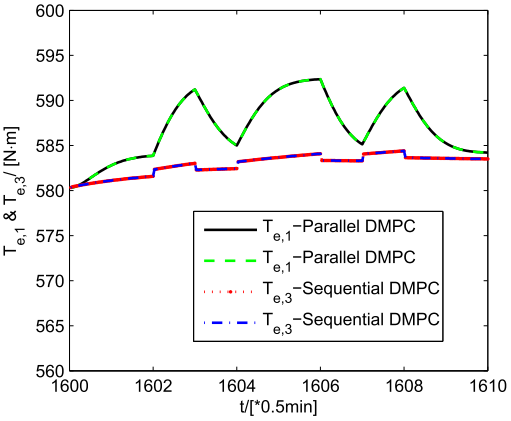

FIGURE 9. Computed torques $T_{e,1}$ and $T_{e,3}$ under sequential distributed MPC and parallel distributed MPC.

are obtained as:

$$B_1 = \begin{bmatrix} 0 & 0 \\ \vdots & \vdots \\ 0 & 0 \\ \frac{q}{J_1} & 0 \\ 0 & \frac{q}{J_2} \\ 0 & 0 \\ \vdots & \vdots \\ 0 & 0 \end{bmatrix} \in R^{10\times2}, \quad B_2 = \begin{bmatrix} 0 & 0 \\ \vdots & \vdots \\ 0 & 0 \\ 0 & 0 \\ 0 & 0 \\ \frac{q}{J_3} & 0 \\ 0 & \frac{q}{J_4} \\ 0 & 0 \end{bmatrix} \in R^{10\times2}.$$

Then, the distributed form (18) of cutterhead is constructed and ready for distributed MPC design.

The parameters of cutterhead systems used in this simulation follow form [5] and are shown in Table 1. The constraints on the states and inputs are $0\ rad/s \leq \omega_m \leq 7\ rad/s$, $0\ N\cdot m \leq T_{e,i} \leq 1500\ N\cdot m$. Random load disturbances are added on the cutterhead system to test the performance robustness of the distributed MPC with respect to the persistent load disturbances. The random load disturbances are

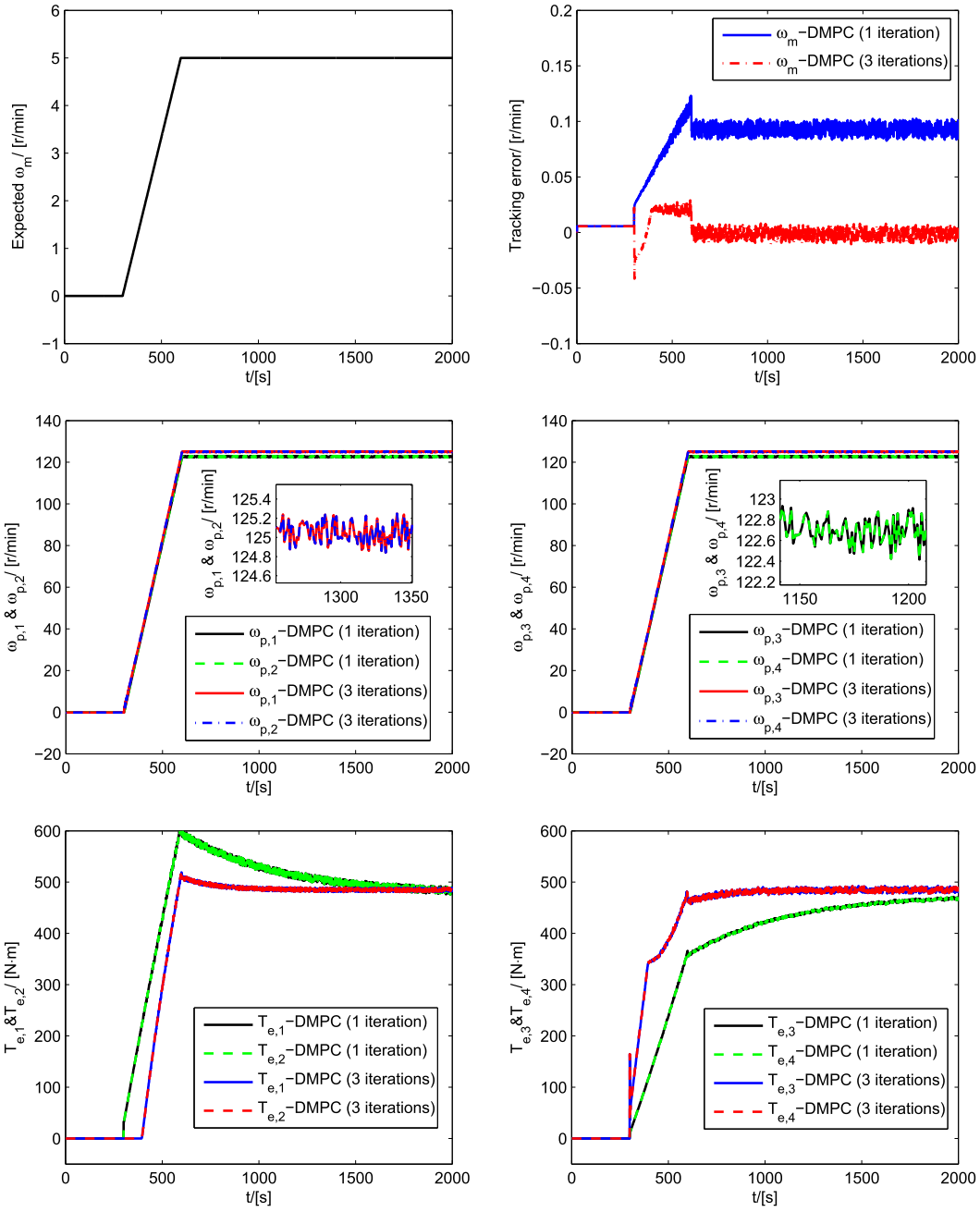

FIGURE 10. Simulation results under the tracking control for SET 2.

described as $T_L = 90 * [1 + 0.25 * (2 * rand - 1)]\ kN \cdot m$, which means that the load changes around 90 $kN \cdot m$ with $\pm 25\%$ fluctuant of load disturbances. The following tracking objective for each subregion is formed:

$$\tilde{J}_{i,k} = \sum_{l=1}^{H_P} \left\| (\omega_{k+l|k} - \omega^r_{k+l|k}) \right\|^2_{Q_y} + \sum_{l=0}^{N-1} \left\| \Delta T_{i,k+l|k} \right\|^2_{R_{i,y}} + \sum_{l=0}^{N-1} \sum_{j=1, j\neq i}^{M} \left\| \Delta T_{j,k+l|k} \right\|^2_{R_{j,y}} \tag{38}$$

The constrained robust distributed MPC is considered with the driving torques can be solved by

$$\min_{\Delta T_{e,i}} J_{i,k} = \left\| \Omega_m(k|k) - \Omega_{m,r}(k|k) \right\|^2_{\hat{Q}_y} + \left\| \Delta T_{e,i}(k|k) \right\|^2_{\hat{R}_i} + \sum_{j=1(j\neq i)}^{M} \left\| \Delta T_{e,i}(k|k) \right\|^2_{\hat{R}_j}$$
$$s.t.\ 0N \cdot m \leq T_{e,i} \leq 1500N \cdot m \tag{39}$$

where $\Omega_m(k|k) = \left[\omega_m^T(k+1|k) \cdots \omega_m^T(k+H_P)\right]^T$ and $\Omega_{m,r}(k|k) = \left[\omega_r^T(k+1|k) \cdots \omega_r^T(k+H_P)\right]^T$.

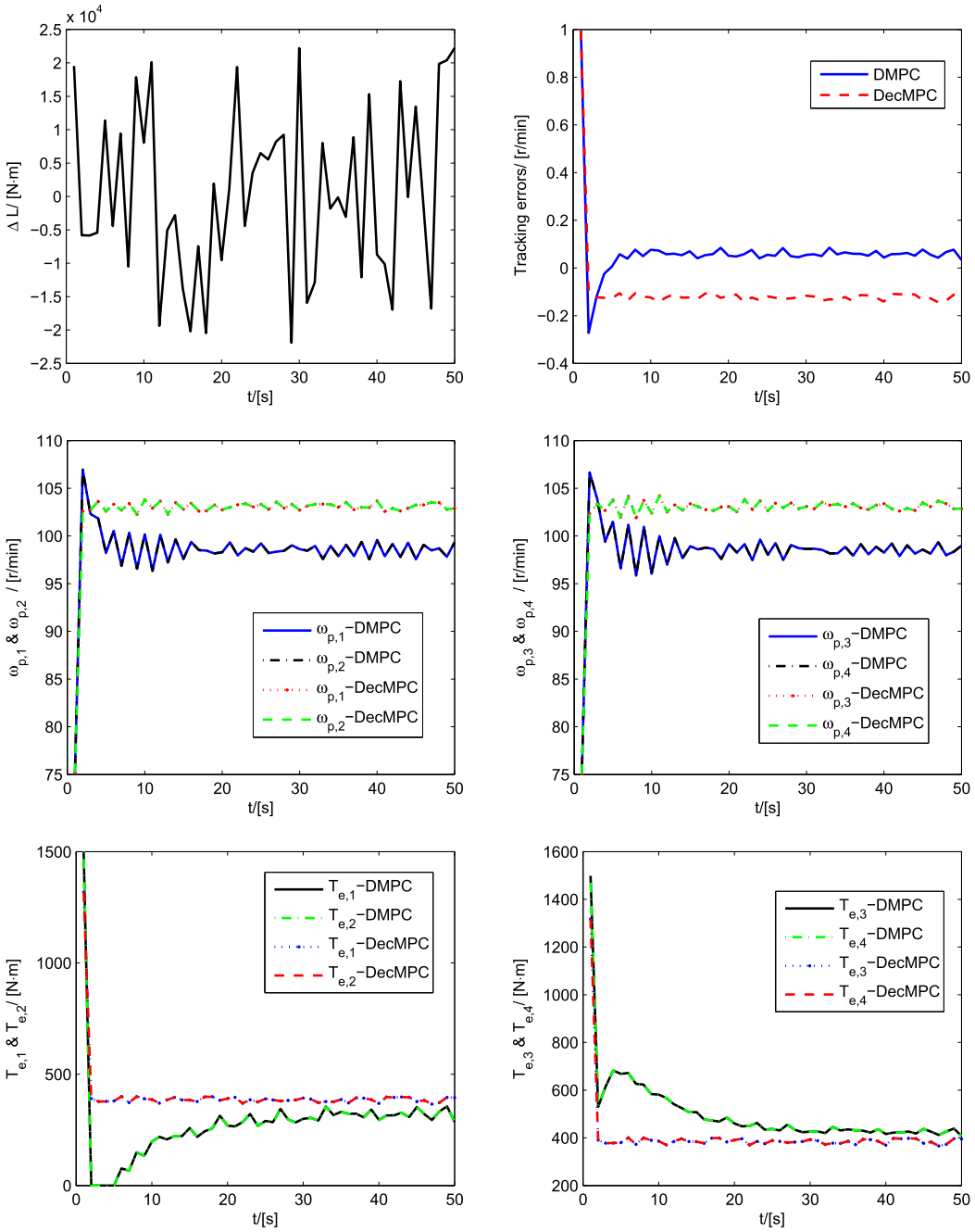

FIGURE 11. Simulation results under the disturbance rejection for SET 3.

Then, the QP solver quadprog function in MATLAB is used to solve the $\Delta T^*_{e,i}$. The required speed is given by the operator by evaluating the excavating environment. The angular velocity of cutterhead system is tracked under distributed MPC. The distributed MPC controllers provide the setpoints $T^*_{e,i}$ for the local PID control layer. The following three cases are discussed in the simulation:

- SET 1: The operation data of 'Yin Song Water Supply Project' in China is used to test the proposed torque optimization of cutterhead system using distributed MPC. The given expected output speed ω_m is used as the settings of the cutterhead system and measured load is injected into the plant to test the performance;
- SET 2: The speed of cutterhead is required to track the given trajectories under the control constraints. The model errors are considered in this case by setting $k_{t,i}$ and $c_{t,i}$ as uncertain parameters. We do this because the linear model is simplified by setting them as average values. It is reasonable to assumed that $k_{t,i} = k_{t,0}[1 + 0.01*(2*rand-1)]$ and $c_{t,i} = c_{t,0}[1+0.01*(2*rand-1)]$, which means that there randomly $\pm 1\%$ fluctuant of these two parameters;

- SET 3: Random load disturbances are added on the cutterhead system to test the performance robustness of the controller to the persistent load disturbances. The random load disturbances are described as $T_L = 90*[1+0.25*(2*rand-1)]\ kN\cdot m$, which means that the load changes around $90\ kN\cdot m$ with $\pm 25\%$ fluctuant of load disturbances.

B. SIMULATION RESULTS

For SET 1, the angular velocity is used as the set-point of the cutterhead system. The load is applied to the system as the additional measurable input. The results are compared with the parallel distributed MPC method. The tracking performance is shown in Fig. 8 and the controller are shown in Fig. 9. The results show that, by using distributed MPC with two iterations, the angular velocity of TBM cutterhead system is well tracked. For the parallel distributed MPC method, since controllers of neighbor subsystems are based on the initial guessed ones, the performance with only two iterations are not enough to ensure the tracking the expected trajectories. This shows that the proposed sequential and iterative method is more easy to achieve better formance with less iterations.

For SET 2, the distributed MPC method is implemented with one iteration and three iterations, respectively. The desired speed ω_m^* tracking performances are shown in Fig. 10, demonstrating the good tracking performance of cutterhead system under distributed MPC. It is found that the tracking error could be $0.1\ r/min$ when the distributed MPC is implemented with only one iteration, which is not acceptable in practice. The proposed distributed MPC controller with three iterations can achieve very small tracking errors, which indicates that the proposed distributed MPC controller can meet the speed control performance requirement in this situation.

For SET 3, simulations are further tested with persistent load disturbances $T_L = 90*[1+0.25*(2*rand-1)]\ kN\cdot m$ added to the cutterhead system. Similarly, the distributed MPC is implemented with three iterations. The simulation results are compared with the decentralized MPC method where the couplings are not considered in the controller design. The results are presented in Fig. 11 and show that the tracking errors meet the requirements under the distributed MPC tracking control, which demonstrate the robustness of the controller to persistent load disturbances. The tracking errors with distributed MPC is much better than the fully decentralized MPC method. The results also show that the constraints $0 \le T_{e,i}(i = 1, 2, 3, 4) \le 1500\ N\cdot m$ of driving torques are all satisfied and the tracking error is acceptable.

V. CONCLUSION

This paper presents the torque optimization framework for multi-motor driving TBM cutterhead system with distributed MPC. A linear dynamic model of TBM cutterhead system is established. A sequential and iterative distributed MPC is proposed for optimizing the input torques of the driving motors. The testing results show the effectiveness of the proposed distributed MPC framework.

ACKNOWLEDGMENT

The authors would like to thank the Editor and the anonymous reviewers for their valuable suggestions and comments.

REFERENCES

[1] J. Huo, N. Hou, W. Sun, L. Wang, and J. Dong, "Analyses of dynamic characteristics and structure optimization of tunnel boring machine cutter system with multi-joint surface," *Nonlinear Dyn.*, vol. 87, no. 1, pp. 237–254, 2017.
[2] D.-W. Lee *et al.*, "Thermal-hydraulic analysis for conceptual design of Korean HCCR TBM set," *IEEE Trans. Plasma Sci.*, vol. 44, no. 9, pp. 1571–1575, Sep. 2016.
[3] L. Wang, G. Gong, H. Yang, X. Yang, and D. Hou, "The development of a high-speed segment erecting system for shield tunneling machine," *IEEE/ASME Trans. Mechatronics*, vol. 18, no. 6, pp. 1713–1723, Dec. 2013.
[4] G.-J. Bae *et al.*, "Manufacturing of an earth pressure balanced shield TBM cutterhead for a subsea discharge tunnel and its field performance analysis," *J. Korean Tunnelling Underground Space Assoc.*, vol. 16, no. 2, pp. 161–172, 2014.
[5] X. H. Li, H. B. Yu, M. Z. Yuan, J. Wang, and Y. Yin, "Dynamic modeling and analysis of shield TBM cutterhead driving system," *J. Dyn. Syst., Meas., Control*, vol. 132, no. 4, 2010, Art. no. 044504.
[6] X. Li, H. Yu, P. Zeng, M. Yuan, J. Han, and L. Sun, "Study on linear vibration model of shield tbm cutterhead driving system," *Int. J. Acoust. Vifibrations*, vol. 19, no. 2, pp. 89–106, 2014.
[7] L. Wang, Y. Kang, X. Zhao, and Q. Zhang, "Disc cutter wear prediction for a hard rock TBM cutterhead based on energy analysis," *Tunnelling Underground Space Technol.*, vol. 50, pp. 324–333, Aug. 2015.
[8] J. Ling, W. Sun, J. Huo, and L. Guo, "Study of TBM cutterhead fatigue crack propagation life based on multi-degree of freedom coupling system dynamics," *Comput. Ind. Eng.*, vol. 83, pp. 1–14, May 2015.
[9] K. Talebi, H. Memarian, J. Rostami, and E. A. Gharahbagh, "Modeling of soil movement in the screw conveyor of the earth pressure balance machines (EPBM) using computational fluid dynamics," *Tunnelling Underground Space Technol.*, vol. 47, pp. 136–142, Mar. 2015.
[10] B. Ding and H. Pan, "Output feedback robust MPC for LPV system with polytopic model parametric uncertainty and bounded disturbance," *Int. J. Control*, vol. 89, no. 8, pp. 1554–1571, 2016.
[11] S. J. Qin and T. A. Badgwell, "A survey of industrial model predictive control technology," *Control Eng. Pract.*, vol. 11, no. 7, pp. 733–764, 2003.
[12] Y. Shi, C. Shen, H. Fang, and H. Li, "Advanced control in marine mechatronic systems: A survey," *IEEE/ASME Trans. Mechatronics*, vol. 22, no. 3, pp. 1121–1131, Jun. 2017.
[13] S. Vazquez *et al.*, "Model predictive control: A review of its applications in power electronics," *IEEE Ind. Electron. Mag.*, vol. 8, no. 1, pp. 16–31, Mar. 2014.
[14] S. Bolognani, S. Bolognani, L. Peretti, and M. Zigliotto, "Design and implementation of model predictive control for electrical motor drives," *IEEE Trans. Ind. Electron.*, vol. 56, no. 6, pp. 1925–1936, Jun. 2009.
[15] G. P. Incremona, A. Ferrara, and L. Magni, "MPC for robot manipulators with integral sliding modes generation," *IEEE/ASME Trans. Mechatronics*, vol. 22, no. 3, pp. 1299–1307, Jun. 2017.
[16] M. Pisaturo, M. Cirrincione, and A. Senatore, "Multiple constrained MPC design for automotive dry clutch engagement," *IEEE/ASME Trans. Mechatronics*, vol. 20, no. 1, pp. 469–480, Feb. 2015.
[17] A. G. Beccuti, S. Mariethoz, S. Cliquennois, S. Wang, and M. Morari, "Explicit model predictive control of DC–DC switched-mode power supplies with extended Kalman filtering," *IEEE Trans. Ind. Electron.*, vol. 56, no. 6, pp. 1864–1874, Jun. 2009.
[18] R. Scattolini, "Architectures for distributed and hierarchical model predictive control—A review," *J. Process Control*, vol. 19, no. 5, pp. 723–731, 2009.
[19] P. D. Christofides, R. Scattolini, D. M. de la Peña, and J. Liu, "Distributed model predictive control: A tutorial review and future research directions," *Comput. Chem. Eng.*, vol. 51, pp. 21–41, Apr. 2013.
[20] L. Magni and R. Scattolini, "Stabilizing decentralized model predictive control of nonlinear systems," *Automatica*, vol. 42, no. 7, pp. 1231–1236, 2006.

[21] S. Riverso, M. Farina, and G. Ferrari-Trecate, "Plug-and-play decentralized model predictive control for linear systems," *IEEE Trans. Autom. Control*, vol. 58, no. 10, pp. 2608–2614, Oct. 2013.

[22] T. H. Mohamed, H. Bevrani, A. A. Hassan, and T. Hiyama, "Decentralized model predictive based load frequency control in an interconnected power system," *Energy Convers. Manage.*, vol. 52, no. 2, pp. 1208–1214, 2011.

[23] A. Alessio, D. Barcelli, and A. Bemporad, "Decentralized model predictive control of dynamically coupled linear systems," *J. Process Control*, vol. 21, no. 5, pp. 705–714, 2011.

[24] M. S. Elliott and B. P. Rasmussen, "Decentralized model predictive control of a multi-evaporator air conditioning system," *Control Eng. Pract.*, vol. 21, no. 12, pp. 1665–1677, 2013.

[25] M. Vaccarini, S. Longhi, and M. R. Katebi, "Unconstrained networked decentralized model predictive control," *J. Process Control*, vol. 19, no. 2, pp. 328–339, 2009.

[26] L. Liang and Y. Wen, "Integrated rudder/fin control with disturbance compensation distributed model predictive control," *IEEE Access*, vol. 6, pp. 72925–72938, 2018.

[27] Z. Cai, H. Zhou, J. Zhao, K. Wu, and Y. Wang, "Formation control of multiple unmanned aerial vehicles by event-triggered distributed model predictive control," *IEEE Access*, vol. 6, pp. 55614–55627, 2018.

[28] W. Al-Gherwi, H. Budman, and A. Elkamel, "Selection of control structure for distributed model predictive control in the presence of model errors," *J. Process Control*, vol. 20, no. 3, pp. 270–284, Sep. 2010.

[29] X. Yin and J. Liu, "Subsystem decomposition of process networks for simultaneous distributed state estimation and control," *AIChE J.*, vol. 65, no. 3, pp. 904–914, 2019.

[30] W. Al-Gherwi, H. Budman, and A. Elkamel, "A robust distributed model predictive control based on a dual-mode approach," *Comput. Chem. Eng.*, vol. 50, pp. 130–138, Mar. 2013.

[31] J. M. Maestre, D. M. de la Peña, E. F. Camacho, and T. Alamo, "Distributed model predictive control based on agent negotiation," *J. Process Control*, vol. 21, no. 5, pp. 685–697, 2011.

[32] S. Li, Y. Zhang, and Q. Zhu, "Nash-optimization enhanced distributed model predictive control applied to the shell benchmark problem," *Inf. Sci.*, vol. 170, nos. 2–4, pp. 329–349, 2005.

[33] I. Alvarado *et al.*, "A comparative analysis of distributed MPC techniques applied to the HD-MPC four-tank benchmark," *J. Process Control*, vol. 21, no. 5, pp. 800–815, 2011.

[34] S. Riverso and G. Ferrari-Trecate, "Tube-based distributed control of linear constrained systems," *Automatica*, vol. 48, no. 11, pp. 2860–2865, 2012.

[35] L. Zhang, J. Wang, and C. Li, "Distributed model predictive control for polytopic uncertain systems subject to actuator saturation," *J. Process Control*, vol. 23, no. 8, pp. 1075–1089, 2013.

[36] J. Liu, D. Muñoz de la Peña, and P. D. Christofides, "Distributed model predictive control of nonlinear systems subject to asynchronous and delayed measurements," *Automatica*, vol. 46, no. 1, pp. 52–61, 2010.

[37] Z. Wang and C. J. Ong, "Distributed model predictive control of linear discrete-time systems with local and global constraints," *Automatica*, vol. 81, pp. 184–195, Jul. 2017.

[38] K. Divya, A.-G. Walid, and B. Hector, "Robust-distributed MPC tolerant to communication loss," *Comput. Chem. Eng.*, vol. 88, pp. 30–38, May 2016.

[39] L. Zhang, J. Wang, and B. Wang, "Distributed MPC of polytopic uncertain systems: Handling quantised communication and packet dropouts," *Int. J. Syst. Sci.*, vol. 46, no. 13, pp. 2393–2406, 2015.

[40] J. Liao, Z. Chen, and B. Yao, "High-performance adaptive robust control with balanced torque allocation for the over-actuated cutter-head driving system in tunnel boring machine," *Mechatronics*, vol. 46, pp. 168–176, 2017.

[41] W. Sun, M. Shi, J. Li, X. Ding, L. Wang, and X. Song, "Surrogate-based multisource sensitivity analysis of TBM driving system," *Shock Vib.*, vol. 2018, May 2018, Art. no. 5187535. doi: 10.1155/2018/5187535.

[42] K. V. Ling, J. Maciejowski, A. Richards, and B. F. Wu, "Multiplexed model predictive control," *Automatica*, vol. 48, no. 2, pp. 396–401, Feb. 2012.

[43] P. O. M. Scokaert, D. Q. Mayne, and J. B. Rawlings, "Suboptimal model predictive control (feasibility implies stability)," *IEEE Trans. Autom. Control*, vol. 44, no. 3, pp. 648–654, Mar. 1999.

XIAOFENG YANG was born in 1976. He received the B.Eng. degree from the Department of Mathematics, Jinan University, Guangzhou, China, in 1998, and the M.S. degree from the Department of Electronics and Information Engineering, Huazhong University of Science and Technology, Wuhan, China, in 2009. He is currently pursuing the Ph.D. degree with the College of Automation Science and Engineering, South China University of Technology.

He was a Systems Engineer with Shenzhen Telecom Group Co., Ltd., from 1998 to 2001. His research interests include model predictive control, robust control, and networked control systems.

LANGWEN ZHANG (M'18) was born in 1986. He received the B.Eng. degree from the College of Automation Science and Technology, South China University of Technology, Guangzhou, China, in 2010, and the Ph.D. degree from the Department of Automation, Shanghai Jiao Tong University, Shanghai, China, in 2015.

From 2015 to 2017, he was a Postdoctoral Fellow with the College of Automation Science and Technology, South China University of Technology. From 2018 to 2019, he was a Visiting Professor with Chemical & Materials Engineering, University of Alberta. He is currently an Assistant Professor with College of Automation Science and Technology, South China University of Technology. His research interests include distributed model predictive control, process control, and multi-agent systems. He was a recipient of the Outstanding Ph.D. Graduate Award from Shanghai, China, in 2015.

WEI XIE was born in 1974. He received the B.S. and M.S. degrees with the Automation Department, Wuhan of Science and Technology, China, 1996 and 1999, respectively, and the Ph.D. degree from the Kitami Institute of Technology, Japan, in 2003. He was a Postdoctoral Researcher with the Satellite Venture Business Laboratory, from 2003 to 2006. In 2006, he joined the College of Automation Science and Engineering, South China University of Technology, as an Associate Professor and was promoted to be a Full Professor in 2010. He is an Inventor/Co-Inventor for China patents. His research interests include robust control theory and application gain scheduling Control, pattern recognition, computer control and application, and video information processing. He has been a Reviewer for several prestigious international journals, including the IEEE TRANSACTION ON AUTOMATIC CONTROL, *IET Control Theory and Applications*, the *International Journal of Control*.

JUNFENG ZHANG received the M.S. degree from the College of Mathematics and Information Science, Henan Normal University, in 2008, and the Ph.D. degree from the School of Electronic Information and Electrical Engineering, Shanghai Jiao Tong University, in 2014.

Since 2014, he has been a Lecturer with the School of Automation, Hangzhou Dianzi University. Since 2017, he has also been an Associate Professor. His research interests include positive systems, switched systems, model predictive control, and differential inclusions. He was a recipient of the Outstanding Master Degree Thesis Award from Henan Province, China, in 2011, and the Outstanding Ph.D. Graduate Award from Shanghai, China, in 2014. He is the Co-Chair of Program Committee in the 6th International Conference on Positive Systems (POSTA2018).